

Rate coefficients in a degenerate plasma produced by short wavelength lasers

Contact: va567@york.ac.uk

V. Aslanyan, G. J. Tallents

York Plasma Institute,
University of York,
YO10 5DD, United Kingdom

Abstract

The electrons in a dense plasma follow Fermi-Dirac statistics, which deviate significantly in this regime from the usual Maxwell-Boltzmann approach used by many models. We have compared the atomic rate coefficients in the two cases and the resulting populations. The discrepancy is small for solid density plasmas close to local thermodynamic equilibrium, but becomes significant if the plasma is irradiated by photoionizing radiation of irradiance greater than approximately 10^{14} W cm $^{-2}$.

1 Introduction

Collisional-radiative models are frequently used to calculate plasma opacities, equations of state and generate emission spectra. Such models assume that the electrons in a plasma are distributed with one or more Maxwellian components, meaning that the rates of atomic processes can be calculated efficiently.

The Fermi-Dirac kinetic energy distribution for an electron temperature T_e and density n_e is given by

$$f_{FD}(\epsilon, T_e) = \frac{G}{n_e} \frac{\sqrt{\epsilon}}{1 + \exp[(\epsilon - \mu)/T_e]}, \quad (1)$$

where $\mu(n_e, T_e)$ is the chemical potential and $G = 4\pi(2m_e/h^2)^{3/2}$, where the constants have their usual meanings. The chemical potential is calculated at each temperature and density from the zeroth moment of the distribution, $\int_0^\infty f_{FD}(\epsilon, T_e)d\epsilon = 1$. The chemical potential decreases monotonically with temperature and tends to an asymptote for which the energy distribution becomes Maxwellian. In practice, this means that the Fermi-Dirac distribution differs significantly from the Maxwell-Boltzmann at low temperatures (< 20 eV) and high densities ($\gtrsim 10^{22}$ cm $^{-3}$). Such densities are higher than the critical density of visible lasers, but may be directly created via ultraviolet or soft x-ray lasers. Low temperature, high density plasmas are also universally present in ultraviolet to infrared laser plasmas between the critical density and the ablation surface.

A degenerate plasma introduces the need to take account of empty energy states when calculating the rates of processes. We model this by the inclusion of Pauli blocking factors, which correspond to the probability

that a quantum state with energy ϵ is available for an emerging electron to occupy, given by

$$\tilde{F}(\epsilon, T_e) = 1 - \{1 + \exp[(\epsilon - \mu)/T_e]\}^{-1}. \quad (2)$$

2 Calculation of the rate coefficients

Calculations of rate coefficients follow the usual approach of integrals over the product of the cross section and energy distributions; $\int_0^\infty \sqrt{2\epsilon/m_e} \sigma f d\epsilon$ for collisional excitation, for example. For a degenerate plasma, we replace the usual Maxwell-Boltzmann distribution $f_{MB}(\epsilon, T_e) = (2/\sqrt{\pi})\sqrt{\epsilon} \exp(-\epsilon/T_e)$ with that of Equation (1) for each incoming electron and add a Pauli blocking factor from Equation (2) for each outgoing electron. This introduces a problem, because integrals of these functions can no longer be carried out analytically; numerical integration is significantly more computationally intensive.

The inclusion of the Pauli blocking factors into the collisional ionization coefficients necessitates the use of the differential cross section, which complicates their calculation. In this process, the remainder of an incoming electron's kinetic energy is shared between two outgoing electrons, both with a corresponding blocking factor; the differential cross section in effect governs how this energy is shared. We have for the collisional ionization coefficient,

$$K_{FD}^\uparrow = N_i G \sqrt{\frac{2}{m_e}} \int_{E_i}^\infty \int_0^{\epsilon_0 - E_i} \epsilon_0 \frac{d\sigma^\uparrow}{d\epsilon_1} \tilde{F}(\epsilon_1, T_e) \times \frac{\tilde{F}(\epsilon_0 - \epsilon_1 - E_i, T_e)}{1 + \exp[(\epsilon_0 - \mu)/T_e]} d\epsilon_0 d\epsilon_1, \quad (3)$$

where E_i is the ionization energy and N_i the ion density. Blocking factors do not appear in classical theory, so the differential cross section may be integrated to directly obtain the total cross section. Therefore, the differential cross section has been poorly studied experimentally. We have extended Mott's differential cross section[1] to be compatible with recently published collisional ionization cross sections.

The inverse rates of collisional processes may be calculated by using appropriate micro-reversibility relations[2]. We have used the standard approach of

grouping the processes into rate matrix, which may be inverted to obtain the steady state or used to solve for the time-dependent ion populations.

3 Steady state ionization

We have used our collisional-radiative model to calculate the steady state ion populations and hence the ionization fraction of carbon for a given total ion density and varying temperature. We have also varied the intensity of incident monochromatic radiation with photon energies of 50 eV; the results are shown in Figure 3. The photoionization cross section generally decreases with photon energy above threshold and hence the rate of photoionization is high for carbon at the selected photon energy.

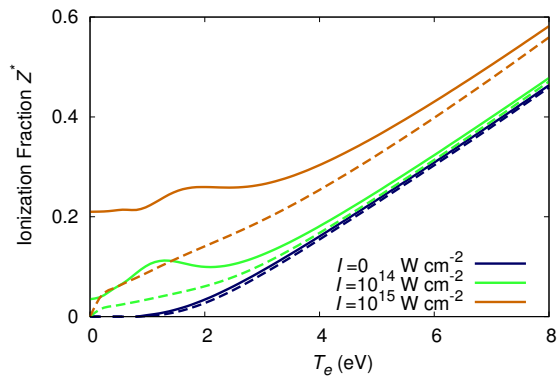


Figure 1: Comparison of the steady state ionization fraction of a carbon plasma (density of 2.23 g cm^{-3} , corresponding to graphite) for Fermi-Dirac (solid) and Maxwell-Boltzmann (dashed) statistics, irradiated by 50 eV photons at intensities indicated.

We see that the impact of the Fermi-Dirac rates is negligible without the incident radiation (where it is approximately in local thermodynamic equilibrium), because the ionization fraction is roughly linear with temperature and so the electron density is never sufficient for the plasma to be degenerate. However, strong photoionization creates a degenerate high electron density, leading to divergence in the two cases.

4 Time evolution

We have calculated the temperature and ionization of carbon, which is taken initially to be fully neutral, with a short incident Gaussian laser pulse of 14 eV photons (just above the first ionization energy of carbon) shown in Figure 4. The temperature was calculated from the absorbed laser energy by inverting the expression for the average energy of an electron, $\varepsilon = \int_0^\infty \epsilon f_{FD}(\epsilon, T_e) d\epsilon$. The temperature and ionization fraction diverge in the

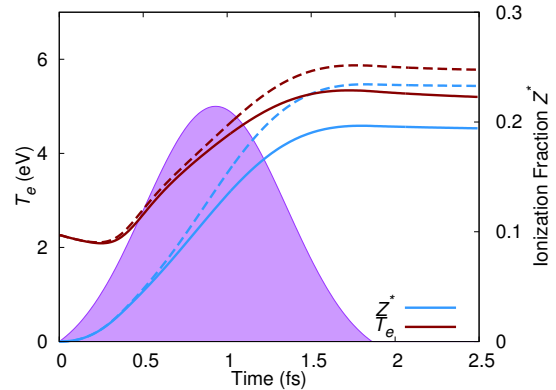


Figure 2: Evolution of the electron temperature and ionization fraction of carbon (density of 3.53 g cm^{-3} , corresponding to diamond) irradiated by a laser beam with photon energies of 14 eV and Gaussian intensity as shown shaded with a full-width half maximum of 1 fs and peak intensity of $10^{14} \text{ W cm}^{-2}$ with Maxwell-Boltzmann (dashed line) and Fermi-Dirac (solid line) statistics as indicated.

two cases, but may begin to match if the pulse were longer and hence the final temperature became higher.

5 Conclusion

We have presented a method for calculating the atomic rates in a plasma described by the Fermi-Dirac distribution and compared properties to those of a classical plasma. We have confirmed that the classical approach for calculating rates is sufficient for most plasmas of interest, but demonstrate that the additional computational effort required to calculate degenerate rate coefficients may be required to simulate a dense plasma created by lasers from the ultraviolet to the soft x-ray.

References

- [1] N. Oda, *Radiation Research* **64**, 80 (1975).
- [2] J. Oxenius, *Kinetic Theory of Particles and Photons: Theoretical Foundations of Non-LTE Plasma Spectroscopy* (Springer-Verlag, 1986).
- [3] V. Aslanyan and G. J. Tallents, *Phys. Rev. E* **91**, 063106 (2015).
- [4] B. Deschaud, O. Peyrusse, and F. B. Rosmej, *EPL* **108**, 53001 (2014).
- [5] B. Deschaud, O. Peyrusse, and F. B. Rosmej, *HEDP* **15**, 22 (2015).